

Synthesis, Structures, and Electrochemical Characteristics of Pyrophosphates

Uebou, Yasushi
Institute of Advanced Material Study Kyushu University

Okada, Shigeto
Institute of Advanced Material Study Kyushu University

Egashira, Minato
Institute of Advanced Material Study Kyushu University

Yamaki, Jun-ichi
Institute of Advanced Material Study Kyushu University

<https://doi.org/10.15017/7937>

出版情報：九州大学機能物質科学研究所報告. 15 (1), pp.57-61, 2001. Institute of Advanced Material Study Kyushu University

バージョン：

権利関係：



Synthesis, Structures, and Electrochemical Characteristics of Pyrophosphates

Yasushi UEBOU, Shigeto OKADA,
Minato EGASHIRA and Jun-ichi YAMAKI

We synthesized the two pyrophosphates LiVP_2O_7 and TiP_2O_7 by a solid state reaction, and the cathode properties of lithium secondary batteries were investigated. The structures were characterized by powder X-ray Rietveld refinement. Lithium cells using LiVP_2O_7 and TiP_2O_7 cathodes showed that approximately 0.5 Li per unit could be reversibly deintercalated from LiVP_2O_7 at 4.1 V vs. Li/Li^+ , 0.8 Li per unit could be reversibly intercalated into TiP_2O_7 at 2.6 V vs. Li/Li^+ . The redox potentials 4.1 V of LiVP_2O_7 and 2.6 V of TiP_2O_7 were higher than that of transition metal oxides such as VO_2 and TiO_2 .

Introduction

Transition metal oxides, such as LiCoO_2 , LiNiO_2 , and LiMn_2O_4 have been investigated extensively as positive electrode materials for "rocking chair" batteries with carbon lithium negative electrodes^{1,2}. At the same time, a number of materials have been synthesized and evaluated for use as the cathode-active material in lithium secondary batteries. Recently, Goodenough *et al.* investigated polyanionic compounds that exhibit framework structures built up from both (MO_n) polyhedra (most often octahedra) and $(\text{XO}_4)^{m-}$ tetrahedra polyanions (M = transition metal; X = P, S, V, As, Mo, W)^{3,4} instead of only (MO_n) polyhedra in transition oxides. Such structures can be viewed as obtained by the replacement of O^{2-} anions by larger size $(\text{XO}_4)^{m-}$ polyanions. Well-known examples of such compounds are: phosphates such as olivine-type LiFePO_4 ³ or NASICON-type $\text{Li}_3\text{Fe}_2(\text{PO}_4)_3$ ³, sulfates such as $\text{Fe}_2(\text{SO}_4)_3$ ⁵ or vanadates such as spinel-type $\text{V}[\text{LiMn}]\text{O}_4$ ⁶.

The synthesis of new NASICON phosphates with mixed conductivity and the Na intercalation properties of such compounds have been studied since the early 90s^{7,8,9}. Li intercalation properties of such compounds have been known for more than ten years^{5,10,11}. Interest has been focused recently on polyanionic compounds as cathode materials of rechargeable Li batteries^{3,4,12,13}. These materials display lower theoretical specific capacities than transition metal oxides, because they contain a "dead mass" coming from the non-electroactive X cations that cannot store electrons. However, they are of high interest because their operating voltage can be monitored in the 2.5 - 4.0V range as a function of the nature of M and X

cations¹³, the choice of the $\text{M}^{\alpha+}/\text{M}^{(\alpha-1)+}$ redox system⁴ and the type of crystal structure³. It has also been shown in previous works on $\text{Li}_x\text{Fe}_2(\text{XO}_4)_3$ (X = Mo, W, S, P)^{3,4} compounds, the $\text{Fe}^{3+}/\text{Fe}^{2+}$ redox couple lies at 3.0, 3.0, 3.6, and 2.8 eV vs. Li/Li^+ . From a viewpoint of crystal structure, for example, the $\text{Fe}^{3+}/\text{Fe}^{2+}$ redox potential vs. Li/Li^+ in four iron phosphates, NASICON-type $\text{Li}_3\text{Fe}_2(\text{PO}_4)_3$ ³, the pyrophosphates LiFeP_2O_7 ³ and $\text{Fe}_4(\text{P}_2\text{O}_7)_3$ ³ and olivine-type LiFePO_4 ³ lies at 2.8, 2.9, 3.0, and 3.5 V; each of these materials has a specific capacity of about 100, 60, 110, and 160mAh/g.³

Although all of these phosphates are used in low-cost, high-voltage rare-metal free cathodes, the theoretical capacity of pyrophosphate $\text{Li}_{1+x}\text{FeP}_2\text{O}_7$ is especially small especially due to the large condensate P_2O_7 polyanion. In order to improve the rechargeable capacity of this pyrophosphate, ion exchanges of Fe in LiFeP_2O_7 were attempted using Ti or V in expectation of the reversible $\text{M}^{4+}/\text{M}^{3+}$ redox reaction in addition to the $\text{M}^{3+}/\text{M}^{2+}$ redox reaction.

In this study, a group of $\text{Li}_x\text{MP}_2\text{O}_7$ (M = V, Ti) pyrophosphates with unknown crystal structures were synthesized and characterized by X-ray diffraction (XRD) measurements. To reveal lithium-insertion/extraction reaction, electrochemical characteristics were also investigated by galvanostatic method.

Experiment

LiVP_2O_7 and TiP_2O_7 were prepared by heating appropriate molar ratios of Li_2CO_3 , V_2O_3 , Ti_2O_3 , and $\text{NH}_4\text{H}_2\text{PO}_4$ (Li_2CO_3 and $\text{NH}_4\text{H}_2\text{PO}_4$: Wako Chemical, >99.0% purity; V_2O_3 , Ti_2O_3 : Furuuchi Chemical, >99.9% purity). These samples were mixed; LiVP_2O_7 was fired under argon gas flow at 527K-1373K for 6-12h, and

Received May 31, 2001

Dedicated to Professor Yukio Nishimura on the occasion of his retirement.

TiP₂O₇ was fired in air at 973K for 12-24h.

X-ray diffraction (XRD) patterns of the powdered samples were obtained with an X-ray diffractometer (Rigaku RINT2100HLR/PC) with Cu K α radiation. The XRD data for Rietveld analysis were collected for 1-2 s at each 0.02° step width over a 2 θ range from 10 to 50°. The structural parameters were refined by Rietveld analysis using the computer program RIETAN97- β ¹⁴⁾. The Rietveld method furnishes the refined lattice parameters and structural parameters directly from whole powder diffraction patterns without separating reflections. This method is useful (I) when single crystals cannot be grown at all, (II) when only twinned samples can be prepared, and (III) when physical and/or chemical properties of single crystal forms differ from those of polycrystalline ones. Recently, the structures of many superconducting compounds were determined using neutron measurements and Rietveld method has been widely used to determine the structures of polycrystalline samples.

In the Rietveld analysis, the residual S_y , is minimized as the least squares refinement:

$$S_y = \sum w_i (y_i - y_{ci})^2$$

where

$$W_i = 1/y_i$$

y_i : observed intensity at the i th step,

y_{ci} : calculated intensity at the i th step,

and the sum is overall data points.

The calculated intensities y_i are determined from the F_K^2 values calculated from the structural model by summing of the calculated contributions from neighboring Bragg reflections plus the background:

$$y_{ci} = s \sum L_K |F_K|^2 \rho(2\theta_i - 2\theta_k) P_K A + y_{bi}$$

where

s : scale factor,

K : Miller indices, $h k l$, for a Bragg reflection,

L_K : Lorentz, polarization, and multiplicity factors,

ρ : reflection profile function,

P_K : preferred orientation function,

A : absorption factor,

F_K : structure factor for the k th Bragg reflection,

y_{bi} : background intensity at the i th step.

The Rietveld refinement process will adjust the refinement parameters until the residual is minimized. The parameters, R_{WP} , R_p , R_1 , R_e , and etc., are suggested for the

indicators. Of these indicators, two indicators are important to judge whether the refinement is convoluted satisfactory. R_{WP} (weight pattern R -factor) is the most meaningful of these R because the numerator is the residual being minimized. Another useful numerical criterion is the goodness of fit, S ($=R_{WP}/R_e$).

$$R_{WP} = \left| \frac{\sum_i w_i (y_i - f_{ci})^2}{\sum_i w_i y_i^2} \right|^{1/2}$$

$$R_e = \left| \frac{N_p - N_r - N_c}{\sum_i w_i y_i^2} \right|^{1/2}$$

$$S = \left| \frac{\sum_i w_i (y_i - y_{ci})^2}{N_p - N_r - N_c} \right|^{1/2}$$

Where

N_p : number of strength datum,

N_r : number of parameters that will refinement,

N_c : number of restrictions.

Electrochemical intercalation and de-intercalation were carried out using lithium cells. The working electrode consisted of a mixture of 75mg samples, 25mg acetylene black (Denki Kagaku Co. Ltd.) and 0.3mg F-210L PTFE Teflon binder (Daikin Industry Ltd.) pressed into a tablet of 15mm diameter under a pressure of 10Mpa. The cells used for the electrochemical tests were constructed in a stainless steel 2032 coin-type configuration (20mm outside diameter and 3.2 mm thickness). The counter electrode was a 15mm diameter and 1.0mm thickness disk of lithium metal foil. The electrolytes we used consisted of a 1 M solutions of LiPF₆ in a 50:50 vol.% mixture of ethylene carbonate (EC) and 1,2 dimethoxycarbonate (DMC) (Tomiyama Co. Ltd.). A microporous polypropylene film (Celgard 3501) was used as a separator. The cell construction was indicated in Fig. 1. The cell was assembled in a argon atmosphere (the dew point was less than -70°C). The current density was calculated based on the cathode area. The electrochemical measurements were carried out at room temperature after standing overnight under zero current flow.

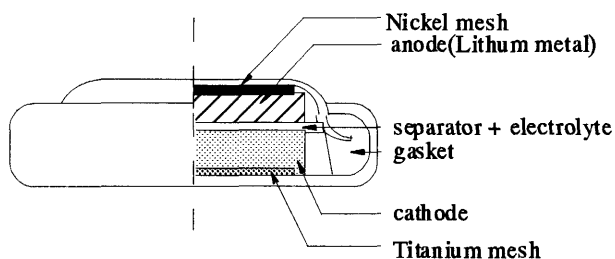


Fig. 1 Lithium cell construction.

Results and Discussion

Synthesis and structures

On indexing the reflection peaks in the powder X-ray pattern of LiVP_2O_7 that was synthesized under argon gas flow at 1373K for 12h, it was found that the sample has a single phase with a monoclinic lattice. We attempted to refine the structure of LiVP_2O_7 using space groups by the Rietveld method. The structure was refined with space group $P2_1$ using a structural model reported by Riou *et al.*¹⁵, that is built up from corner-sharing VO_6 octahedra and P_2O_7 groups. The tunnels result from stacking of rings formed by the edges of three octahedra and four tetrahedra. The overall thermal parameters B for all sites were constrained to be the same value. The lattice parameters was indexed by a monoclinic cell with $a = 4.8102(7)\text{Å}$, $b = 8.1208(5)\text{Å}$, $c = 6.9465(10)\text{Å}$, $\beta = 109.006(10)^\circ$.

On the other hand, TiP_2O_7 was synthesized in air at 973K for 24h. Approximate XRD peaks could be indexed by a cubic lattice similar to that of ZrV_2O_7 ¹⁶ that show complex patterns consistent with the $Pa3$ space group and the $3 \times 3 \times 3$ superstructure, that is built up from corner-sharing ZrO_6 octahedra and V_2O_7 groups. The lattice parameters was indexed by a cubic cell with $a = 23.626(4)\text{Å}$, $Z = 108$. The structures of LiVP_2O_7 and TiP_2O_7 that had been calculated by Rietveld refinement was indicated in Fig. 2(a), (b). The fitting patterns refined best on space group are illustrated in Fig. 3(a), (b). The final R factors, lattice and structural parameters, and their estimated standard deviations were listed on Table 1-2.

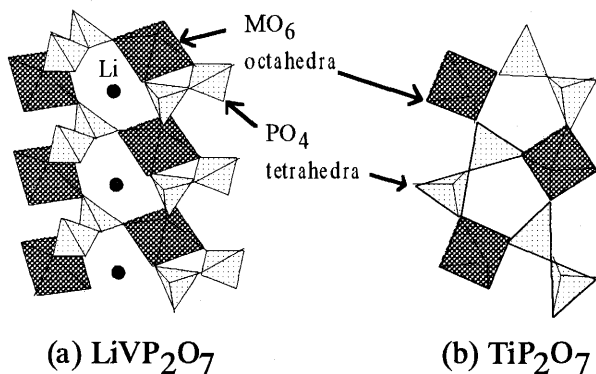


Fig. 2 Crystal structures of (a): LiVP_2O_7 and (b): TiP_2O_7 .

Table 1 X-ray Rietveld refinement results for monoclinic LiVP_2O_7 .^a

Atom	x	y	z	$B(\text{Å}^2)$
Li	0.803(2)	0.384(3)	0.819(2)	$B(V)$
V	0.213(7)	0.236(4)	0.228(8)	0.47(2)
P(1)	0.789(7)	0.455(2)	0.415(13)	$B(V)$
P(2)	0.602(8)	0.051(6)	0.981(5)	$B(V)$
O(1)	0.396(2)	0.079(6)	0.109(7)	$B(V)$
O(2)	0.801(2)	0.209(6)	0.019(16)	$B(V)$
O(3)	0.134(7)	0.056(6)	0.384(3)	$B(V)$
O(4)	0.049(4)	0.423(6)	0.356(5)	$B(V)$
O(5)	0.244(7)	0.394(4)	0.011(17)	$B(V)$
O(6)	0.389(3)	0.100(5)	0.750(5)	$B(V)$
O(7)	0.604(3)	0.319(8)	0.413(4)	$B(V)$

^a Space group: $P2_1$; $a=4.8102(7)\text{Å}$; $b=8.1208(5)\text{Å}$; $c=6.9465(10)\text{Å}$; $\beta=109.006(10)^\circ$; $R_{wp}=14.13\%$; $R_c=8.76\%$; $R_1=4.06\%$, and $S=1.6137$.

Table 2 X-ray Rietveld refinement results for cubic TiP_2O_7 .^b

Atom	x	y	z	$B(\text{Å}^2)$
Ti(1)	0.323(3)	-0.004(6)	0.986(3)	0.7(2)
Ti(2)	0.334(18)	0.350(8)	0.001(9)	$=B(\text{Ti1})$
Ti(3)	0.999(6)	0.333(4)	0.642(6)	$=B(\text{Ti1})$
Ti(4)	0.338(9)	0.666(3)	0.335(9)	$=B(\text{Ti1})$
Ti(5)	0.368(4)	0.368(4)	0.368(4)	$=B(\text{Ti1})$
Ti(6)	0.000	0.000	0.000	$=B(\text{Ti1})$
P(1)	0.458(7)	0.121(7)	0.148(7)	$=B(\text{Ti1})$
P(2)	0.602(8)	0.051(6)	0.981(5)	$=B(\text{Ti1})$
P(3)	0.786(6)	0.127(5)	0.144(16)	$=B(\text{Ti1})$
P(4)	0.779(8)	0.787(8)	0.158(16)	$=B(\text{Ti1})$
P(5)	0.135(7)	0.473(9)	0.794(6)	$=B(\text{Ti1})$
P(6)	0.129(10)	0.789(2)	0.468(2)	$=B(\text{Ti1})$
P(7)	0.452(5)	0.797(5)	0.445(7)	$=B(\text{Ti1})$
P(8)	0.479(3)	0.808(4)	0.781(2)	$=B(\text{Ti1})$
P(9)	0.823(8)	0.823(8)	0.823(8)	$=B(\text{Ti1})$
P(10)	0.457(8)	0.457(8)	0.457(8)	$=B(\text{Ti1})$
P(11)	0.104(13)	0.130(7)	0.141(6)	$=B(\text{Ti1})$
O(1)	0.516(9)	0.181(8)	0.157(5)	$=B(\text{Ti1})$
O(2)	0.847(8)	0.149(7)	0.164(5)	$=B(\text{Ti1})$
O(3)	0.499(7)	0.494(2)	0.192(13)	$=B(\text{Ti1})$
O(4)	0.049(4)	0.423(6)	0.356(5)	$=B(\text{Ti1})$
O(5)	0.162(7)	0.162(7)	0.162(7)	$=B(\text{Ti1})$
O(6)	0.500	0.500	0.500	$=B(\text{Ti1})$
O(7)	0.222(18)	-0.001(6)	0.164(9)	$=B(\text{Ti1})$
O(8)	0.478(5)	0.083(5)	0.146(2)	$=B(\text{Ti1})$
O(9)	0.148(5)	0.406(7)	0.132(8)	$=B(\text{Ti1})$
O(10)	0.142(3)	0.070(12)	0.485(17)	$=B(\text{Ti1})$
O(11)	0.483(8)	0.404(9)	0.135(18)	$=B(\text{Ti1})$
O(12)	0.464(3)	0.075(4)	0.466(2)	$=B(\text{Ti1})$
O(13)	0.154(6)	0.398(9)	0.461(6)	$=B(\text{Ti1})$
O(14)	0.490(9)	0.361(3)	0.460(6)	$=B(\text{Ti1})$
O(15)	0.811(8)	0.086(2)	0.143(9)	$=B(\text{Ti1})$
O(16)	0.146(7)	0.731(2)	0.128(2)	$=B(\text{Ti1})$
O(17)	0.148(3)	0.071(8)	0.805(9)	$=B(\text{Ti1})$

O(18)	0.807(6)	0.751(4)	0.133(3)	=B(Ti1)
O(19)	0.818(5)	0.067(8)	0.777(14)	=B(Ti1)
O(20)	0.122(18)	0.794(18)	0.808(6)	=B(Ti1)
O(21)	0.834(4)	0.689(6)	0.829(6)	=B(Ti1)
O(22)	0.122(9)	0.389(11)	0.813(9)	=B(Ti1)
O(23)	0.147(16)	0.740(5)	0.468(4)	=B(Ti1)
O(24)	0.487(6)	0.740(7)	0.157(2)	=B(Ti1)
O(25)	0.477(3)	0.699(7)	0.558(7)	=B(Ti1)
O(26)	0.480(2)	0.401(3)	0.820(11)	=B(Ti1)
O(27)	0.492(7)	0.736(2)	0.795(9)	=B(Ti1)
O(28)	0.490(8)	0.073(6)	0.793(8)	=B(Ti1)
O(29)	0.796(2)	0.092(3)	0.477(8)	=B(Ti1)
O(30)	0.817(3)	0.443(2)	0.145(3)	=B(Ti1)
O(31)	0.796(9)	0.397(5)	0.469(3)	=B(Ti1)
O(32)	0.799(4)	0.400(4)	0.780(7)	=B(Ti1)
O(33)	0.821(5)	0.745(4)	0.462(9)	=B(Ti1)

^b Space group: *Pa*3; *a*=23.626(4) Å; *R*_w=11.97%;
*R*_c=6.32%, and *S*=1.8927.

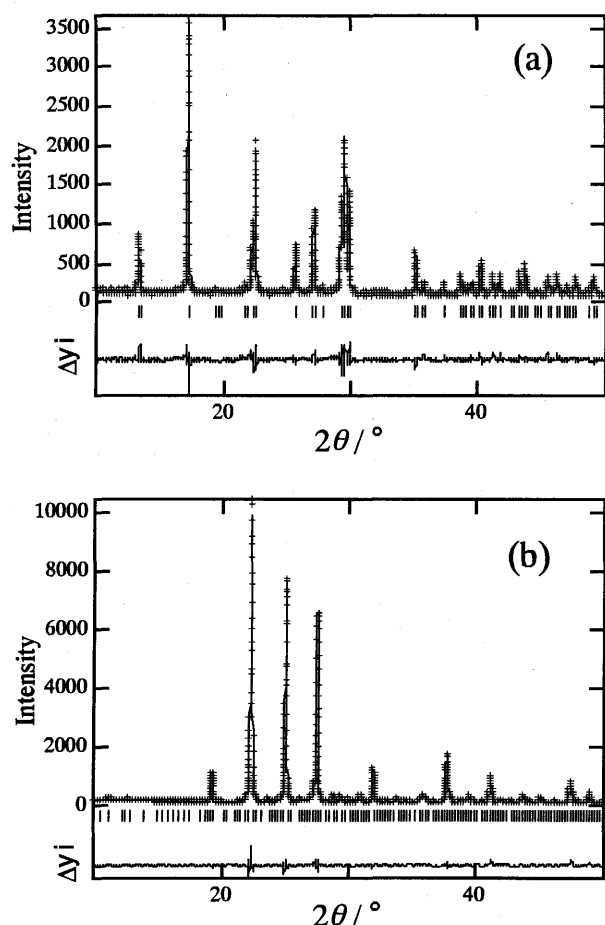


Fig. 3 Observed, calculated and difference plots for X-ray diffraction patterns of (a): LiVP₂O₇ and (b): TiP₂O₇. The solid line is calculated intensity, dots overlying them are observed intensity, and Δ*y*_{*i*} is the difference between observed and calculated intensity.

Electrochemical properties

Fig. 4-5 showed a quasi-open circuit voltage curves for a Li/LiVP₂O₇ and Li/TiP₂O₇ cell. The quasi-open circuit voltage (QOCV) was measured after cell had been standing for 30 minutes at zero current flow for every 0.025 Li/mol depth of charge and discharge at 0.2mA/cm². The lithium content of material indicated in the figure was calculated from electrochemically. In the case of LiVP₂O₇, cell cycling began with lithium extraction, because this sample has lithium ions in the matrix. The extraction of lithium from Li_{1-x}VP₂O₇ proceeded from *x* = 0 to 0.6 with a two-phase reaction which is indicated by the flat charge curve. The curve showed a slope change around *x* = 0.6 to 1.0, which suggests a change in the de-intercalation mechanism. And the compound shows plateau around 4.1V vs. Li/Li⁺ upon discharging. The charge capacity for the first cycle was 115mAh/g, and the discharge capacity was 60mAh/g. The capacity loss could be caused by a decomposition of the electrolytes or a decomposition of the structure of LiVP₂O₇ after the first charge cycle. On the other hand, cell cycling of TiP₂O₇ began with lithium insertion, because this sample has no lithium ions in the matrix. Li/TiP₂O₇ cell showed plateau that was caused by two-phase reaction around 2.6V vs. Li/Li⁺ upon discharging. The discharge capacity for the first cycle was 95mAh/g, and the obtained capacity loss was not much greater than that for the Li/LiVP₂O₇ cell. Although the obtained capacities were lower than expected for large reversible capacity of more than 1Li per in LiMP₂O₇, it is noteworthy that the redox potentials 4.1 V of LiVP₂O₇ and 2.6 V of TiP₂O₇ were higher than that of transition metal oxides. For example, the redox potentials of V⁴⁺/V³⁺ in VO₂¹⁷⁾ is 2.5 V, and that of Ti⁴⁺/Ti³⁺ in TiO₂¹⁷⁾ is 1.8 V.

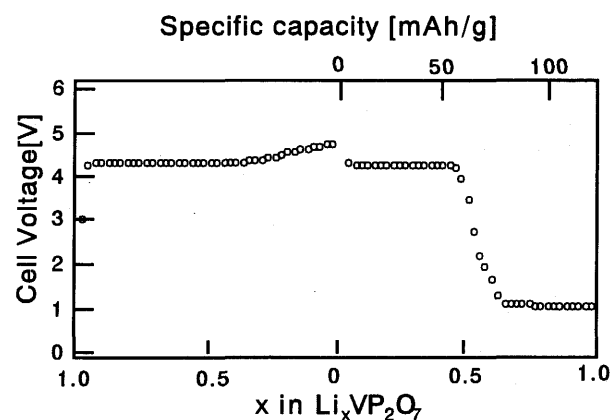


Fig. 4 Quasi-open circuit voltage profile of LiVP₂O₇.

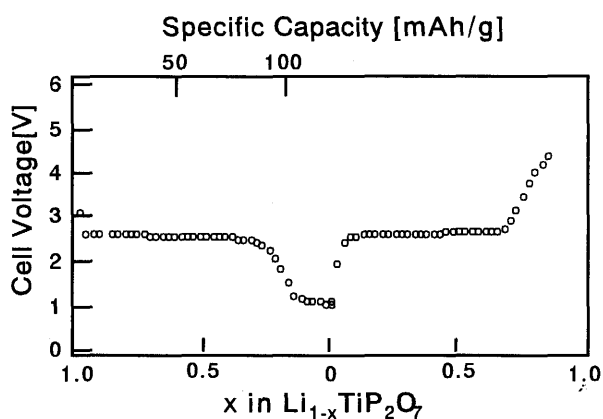


Fig. 5 Quasi-open circuit voltage profile of TiP_2O_7 .

Conclusion

Two pyrophosphates LiVP_2O_7 and TiP_2O_7 were prepared by a solid state reaction. We made two crystal structures clear by Rietveld refinement. The structure of LiVP_2O_7 was isostructural with $P2_1$ monoclinic LiFeP_2O_7 , with $a = 4.8102(7) \text{ \AA}$, $b = 8.1208(5) \text{ \AA}$, $c = 6.9465(10) \text{ \AA}$, and $\beta = 109.006(10)^\circ$. On the other hand, TiP_2O_7 was isostructural with $Pa3$ cubic ZrV_2O_7 , with $a = 23.626(4) \text{ \AA}$. Both structures consist of corner-sharing MO_6 octahedra and P_2O_7 diphosphates. Electrochemical measurements revealed that the two pyrophosphates were suitable as cathode active materials for lithium secondary batteries, and that the redox potentials in these pyrophosphates were higher than that of transition metal oxides such as TiO_2 and VO_2 .

Acknowledgements

The present work was partially supported by Grant-in-Aid for the Development of Innovative Technology from the Ministry of Education, Culture, Sports, Science and Technology of Japan. The authors are grateful to Prof. I. Mochida and Prof. Y. Korai of Kyushu University for their generous support of our XRD measurement.

References

1. K. Tozawa, in *Proceedings of Rechargeable Batteries Conference*, Tokyo, March 3-5, 1990.
2. J.R. Dahn, U. von Sacken, and R. Fong, Abstract 42, p. 66, The Electrochemical Society Meeting Abstracts, vol. 90-2, Seattle, WA, Oct 14-19, 1990.
3. A.K. Padhi, K.S. Nanjundaswamy, C. Masquelier, S. Okada and J.B. Goodenough, *J. Electrochem Soc.*, **144**, 1609 (1997).
4. A.K. Padhi, K.S. Nanjundaswamy, C. Masquelier, and J.B. Goodenough, *J. Electrochem Soc.*, **144**, 2581 (1997).
5. A. Manthiran and J.B. Goodenough, *J. Power Sourc*

es., **26**, 403 (1989).

6. A.K. Padhi, W.B. Archibald, K.S. Nanjundaswamy and J.B. Goodenough, *J Solid State Chem.*, **128**, 267 (1997).
7. O. Tillement, J.C. Couturier, J. Angenault and M. Quarton, *Solid State Ionics*, **48**, 249 (1991).
8. O. Tillement, J. Angenault J.C. Couturier and J.M. Quarton, *Solid State Ionics*, **53-56**, 391 (1992).
9. L. Znaidi, S. Launay and M. Quarton, *Solid State Ionics*, **93**, 273 (1997).
10. A. Nadiri and C. Delmas, *C.R.Acad. Sci. Paris.*, **304** (II), 415 (1987).
11. I. Bussereau, R. Olazcuaga, J.M. Dance and C. Delmas, *J. Alloy & Compounds.*, **188**, 110 (1992).
12. A.K. Padhi, K.S. Nanjundaswamy, S. Okada and J.B. Goodenough, *J. Electrochem. Soc.*, **144**, 1188 (1997).
13. K.S. Nanjundaswamy, A.K. Padhi, J.B. Goodenough, S. Okada, H. Ohtsuka, H. Arai and J. Yamaki, *J. Solid State Ionics*, **92**, 1 (1996).
14. F. Izumi, in *the Rietveld Methode*, R. A Young, Editors, Chap. 13, Oxford Univ. Press, Oxford (1993).
15. D. Rieu, N. Nguyen, R. Benloucif and B. Raveau, *Mat. Res. Bull.*, **25**, 1363 (1990).
16. N. Khosrovani and A. W. Sleight, *J. Solid State Chem.*, **132**, 355 (1997).
17. T. Ohzuku, K. Sawai, and T. Hirai, *Denchi Gijutsu (Battery Technology)*, **3**, 14 (1991).